

1 **The citrate transporter SLC13A5 as a therapeutic target for kidney disease:**  
2 **evidence from Mendelian randomization to inform drug development**

3  
4 Dipender Gill BMBCh PhD<sup>1,2</sup>, Loukas Zagkos PhD<sup>1</sup>, Rubinder Gill MSc<sup>2</sup>, Thomas Benzing  
5 MD<sup>3,4</sup>, Jens Jordan MD<sup>5,6</sup>, Andreas L. Birkenfeld MD<sup>7-9</sup>, Stephen Burgess PhD<sup>10</sup>, Grit Zahn  
6 PhD<sup>11</sup>

- 7
- 8 1. Department of Epidemiology and Biostatistics, School of Public Health, Imperial College  
9 London, London, United Kingdom.
  - 10 2. Primula Group Ltd, London, United Kingdom.
  - 11 3. Department II of Internal Medicine and Center for Molecular Medicine Cologne (CMMC),  
12 University of Cologne, Faculty of Medicine and University Hospital Cologne, Cologne,  
13 Germany.
  - 14 4. Cologne Excellence Cluster on Cellular Stress Responses in Aging-Associated Diseases  
15 (CECAD), University of Cologne, Germany.
  - 16 5. Institute of Aerospace Medicine, German Aerospace Center (DLR), Cologne, Germany.
  - 17 6. Medical Faculty, University of Cologne, Cologne, Germany.
  - 18 7. Department of Diabetology Endocrinology and Nephrology, Internal Medicine IV, University  
19 Hospital Tübingen, Eberhard Karls University Tübingen, Tübingen, Germany.
  - 20 8. Division of Translational Diabetology, Institute of Diabetes Research and Metabolic Diseases  
21 (IDM) of the Helmholtz Center Munich, Eberhard Karls University Tübingen, Tübingen,  
22 Germany, a partner of the German Center for Diabetes Research (DZD e.V.).
  - 23 9. Department of Diabetes, School of Life Course Science and Medicine, King's College London,  
24 London, United Kingdom.

25 10. Medical Research Council Biostatistics Unit at the University of Cambridge, Cambridge,  
26 United Kingdom.

27 11. Eternygen GmbH, Berlin, Germany.

28

29 **Corresponding author details:**

30 Dr Dipender Gill

31 Department of Epidemiology and Biostatistics, School of Public Health, Imperial College London,  
32 London, United Kingdom

33 Telephone: +44 7904843810

34 E-mail: [dipender.gill@imperial.ac.uk](mailto:dipender.gill@imperial.ac.uk)

35

36

37 **Manuscript word count: 3,792**

38 **Abstract** (346 words)

39 Background: Solute carrier family 13 member 5 (SLC13A5) is a Na<sup>+</sup>-coupled citrate co-transporter  
40 that mediates entry of extracellular citrate into the cytosol. SLC13A5 inhibition has been proposed as  
41 a target for reducing progression of kidney disease. The aim of this study was to leverage the  
42 Mendelian randomization paradigm to gain insight into the effects of SLC13A5 inhibition in humans,  
43 towards prioritizing and informing clinical development efforts.

44 Methods: The primary Mendelian randomization analyses investigated the effect of SLC13A5  
45 inhibition on measures of kidney function, including creatinine and cystatin C based measures of  
46 estimated glomerular filtration rate (creatinine-eGFR and cystatin C-eGFR), blood urea nitrogen  
47 (BUN), urine albumin-creatinine ratio (uACR), and risk of chronic kidney disease and  
48 microalbuminuria. Secondary analyses included a paired plasma and urine metabolome-wide  
49 association study, investigation of secondary traits related to SLC13A5 biology, a phenome-wide  
50 association study (PheWAS), and a proteome-wide association study. All analyses were compared to  
51 the effect of genetically predicted plasma citrate levels using variants selected from across the  
52 genome, and statistical sensitivity analyses robust to the inclusion of pleiotropic variants were also  
53 performed. Data were obtained from large scale genetic consortia and biobanks, with sample sizes  
54 ranging from 5,023 to 1,320,016 individuals.

55 Results: We found evidence of associations between genetically proxied SLC13A5 inhibition and  
56 higher creatinine-eGFR ( $p=0.002$ ), cystatin C-eGFR ( $p=0.005$ ), and lower BUN ( $p=3\times 10^{-4}$ ). Statistical  
57 sensitivity analyses robust to the inclusion of pleiotropic variants suggested that these effects may be  
58 a consequence of higher plasma citrate levels. There was no strong evidence of associations of  
59 genetically proxied SLC13A5 inhibition with uACR or risk of CKD or microalbuminuria. Secondary  
60 analyses identified evidence of associations with higher plasma calcium levels ( $p=6\times 10^{-13}$ ) and lower  
61 fasting glucose ( $p=0.02$ ). PheWAS did not identify any safety concerns.

62 Conclusions: This Mendelian randomization analysis provides human-centric insight to guide clinical  
63 development of an SLC13A5 inhibitor. We identify plasma calcium and citrate as biologically plausible  
64 biomarkers of target engagement, and plasma citrate as a potential biomarker of mechanism of  
65 action. Our human genetic evidence corroborates evidence from various animal models to support  
66 effects of SLC13A5 inhibition on improving kidney function.

67

68 **Keywords**

69 SLC13A5, citrate, kidney, renal function, Mendelian randomization, drug development

## 70 **Background**

71 The kidney is a highly metabolically active organ. The provision of citric acid cycle intermediates has  
72 ameliorated renal tubular damage and progression of chronic renal injury in animal models [1–3].  
73 Solute carrier family 13 member 5 (SLC13A5), which is primarily expressed in hepatocytes of the liver,  
74 is a membrane-bound Na<sup>+</sup>-coupled co-transporter responsible for moving extracellular citrate into  
75 the cytosol [4,5]. Systemic SLC13A5 inhibition could augment citrate flux to the kidney, thereby  
76 supporting renal energy metabolism. Moreover, given the role of citrate in regulating glucose  
77 metabolism, lipid metabolism, and inflammation, SLC13A5 inhibition could indirectly affect renal  
78 health [6–13]. However, no SLC13A5 inhibitor has yet entered clinical study, and so evidence of its  
79 efficacy for ameliorating progression of kidney disease in humans is limited. Additionally, SLC13A5  
80 shows species-specific effects [11,14–16].

81 Insights from human genetic data offer a powerful opportunity to prioritize and inform the design of  
82 clinical research. Given that learnings from such genetic analyses relate to the target organism,  
83 namely humans, they are well-placed to overcome some of the limitations of translating findings  
84 from animal models [17]. As genes code for proteins and proteins make up the majority of drug  
85 targets, it follows that naturally occurring variation in the genes coding for drug target proteins can  
86 be leveraged to inform on the effect of their pharmacological perturbation [18]. The random  
87 allocation of genetic variants at conception means that their association with clinical traits and  
88 phenotypes are less susceptible to the confounding factors and reverse causation bias that can  
89 hinder causal inference in traditional epidemiological study designs. The current availability of  
90 publicly accessible large-scale genetic association data also means that such a drug-target Mendelian  
91 randomization paradigm is a relatively fast and cost-effective approach for inferring the potential  
92 clinical effects of perturbing drug targets [19].

93 Given the pre-clinical evidence supporting potential therapeutic applications of SLC13A5 inhibition  
94 [10,12,13,20,21], we sought to investigate its effects using drug target Mendelian randomization. By

95 utilizing the known effect of SLC13A5 inhibition on increasing plasma citrate levels to identify genetic  
96 instruments [10,22,23], our primary objective was to investigate its effects on parameters of kidney  
97 function. In secondary analyses, we aimed to unravel potential mechanisms of action, as well as  
98 evidence of broader effects on glucose and lipid metabolism, and inflammation. Such insights would  
99 thus serve to inform and prioritize clinical development efforts for SLC13A5 inhibitors.

## 100 **Methods**

### 101 ***Study design overview***

102 Genetic instruments for SLC13A5 inhibition were first identified as minimally correlated ( $r^2 < 0.1$ )  
103 single-nucleotide polymorphisms (SNPs) within 200kB of the *SLC13A5* gene (chromosome 17, base  
104 position 6,588,032 to 6,616,886 on reference panel GRCh37/hg19 by Ensembl) that associate with  
105 plasma citrate levels at a genome-wide significance level ( $p < 5 \times 10^{-8}$ ). The inhibition of SLC13A5 would  
106 decrease the transport of citrate from the extracellular to the intracellular compartment. Thus,  
107 variants in *SLC13A5* that are associated with increased levels of plasma citrate may represent greater  
108 inhibition of SLC13A5. A relatively relaxed pruning threshold was used to maximise statistical power,  
109 as the selected genetic variants are confined to only the *SLC13A5* gene region. As a sensitivity check,  
110 the primary analyses were repeated using a more stringent pruning threshold of  $r^2 < 0.01$ . Instrument  
111 validity was tested by performing Mendelian randomization to explore associations with plasma  
112 calcium levels, whose levels are postulated to be increased with SLC13A5 inhibition due to reduced  
113 sequestration in the bone [24]. Such an association would also support plasma calcium as a  
114 biomarker of target engagement for SLC13A5 inhibition.

115 To explore potential mechanisms by which the variants selected as instruments for SLC13A5  
116 inhibition may be exerting their effects, they were functionally annotated using the PhenoScanner  
117 resources (version 2) [25]. The same resource was used to explore potential pleiotropic associations  
118 of any of these variants, by testing for associations with any phenotypes at  $p < 5 \times 10^{-5}$ , which is the  
119 recommended significance threshold to correct for the 1490 tested traits.

120 Primary Mendelian randomization analyses were then performed to investigate the association of  
121 genetically proxied SLC13A5 inhibition with creatinine and cystatin C based measures of estimated  
122 glomerular filtration rate (eGFR), blood urea nitrogen (BUN), urine albumin-creatinine-ratio (uACR),  
123 and risk of microalbuminuria and chronic kidney disease (CKD).

124 To investigate whether any effect of SLC13A5 inhibition on parameters of kidney function may be  
125 attributable to metabolic effects in the plasma that consequently affect kidney function,  
126 metabolome-wide Mendelian randomization of the plasma and urine was undertaken for SLC13A5  
127 inhibition. Evidence of concordant effects of SLC13A5 inhibition on biomarkers measured in the  
128 plasma and urine would be consistent with metabolic effects resulting in compensatory mechanisms  
129 in the kidney, whereas evidence of contrasting effects in the plasma and urine would suggest a  
130 process specific to the kidney underlying the effects.

131 Secondary Mendelian randomization analyses were performed to explore the human genetic  
132 evidence for effects of SLC13A5 inhibition on biomarkers of glucose and lipid metabolism, and  
133 inflammation, namely plasma low-density lipoprotein cholesterol (LDLc), high-density lipoprotein  
134 cholesterol (HDLc), triglycerides, fasting glucose, interleukin 6 (IL6) and C-reactive protein (CRP).  
135 Finally, given that SLC13A5 is predominantly expressed in the liver and is involved in glucose and lipid  
136 metabolism [10,12,20,26], we also investigated potential effects on liver fat.

137 In order to gain potential insight into mediating mechanisms and pathways implicated in the effects  
138 of SLC13A5 inhibition, we also performed a proteome-wide Mendelian randomization study. This  
139 could serve to identify protein mediators for the effect of SLC13A5, as well as potential novel  
140 biomarkers of target engagement. Finally, to investigate potential on-target adverse effects or novel  
141 indications, we performed a phenome-wide association study (PheWAS) [27].

142 To explore whether plasma citrate is a potential mediating mechanism for any associations identified,  
143 and thus could serve as a biomarker of mechanism of action, all analyses that considered genetically  
144 proxied SLC13A5 as the exposure were also repeated for genetically predicted plasma citrate levels,  
145 by selecting instruments from throughout the genome rather than confined to the *SLC13A5* gene  
146 region.

147 A schematic figure depicting the overall study design is presented in Figure 1.



148

149 **Statistical analysis**

150 *Instrument strength*

151 Instrument strength was estimated by calculating the F-statistic for each SNP using the chi-squared  
152 approximation, which for each variant is the square of the SNP-exposure association estimate divided  
153 by the square of the SNP-exposure association estimate's standard error [28].

154

155 *Mendelian randomization*

156 The genome-wide association study summary data sources used for the Mendelian randomization  
157 analyses are presented in Table 1 [29–39]. Participant consent and ethical approval for all data were  
158 obtained in the original studies.

159 The main Mendelian randomization analyses were performed using the random-effects inverse-  
160 variance weighted (IVW) method [40]. This meta-analyses the Wald ratio estimates for each  
161 instrument SNP using a random-effects inverse-variance model. After harmonising SNPs by their  
162 effect alleles, the Wald ratio estimate is calculated by dividing the SNP-exposure association estimate  
163 by the SNP-outcome association estimate. The standard error of the Wald ratio estimate was  
164 calculated using the propagation of error method.

165 Two Mendelian randomization statistical sensitivity analyses were employed, Egger and weighted  
166 median, which make distinct assumptions regarding the inclusion of pleiotropic variants. The Egger  
167 method regresses the SNP-outcome association estimates on the SNP-exposure association  
168 estimates [41]. The slope of the regression provides a Mendelian randomization estimate that is  
169 corrected for pleiotropic associations of the genetic variants and the intercept serves as a test for the  
170 presence of such pleiotropic associations, provided that the magnitudes of these pleiotropic  
171 associations are not correlated to instrument strength. The weighted median method orders the

172 Wald ratio estimates for all instrument SNPs weighted by their precision, and selects the median  
173 value, with 95% confidence intervals (95% CIs) calculated by bootstrapping [42]. It provides an  
174 accurate Mendelian randomization estimate when more than half the information for the analysis  
175 comes from valid instruments. Heterogeneity in MR estimates derived from individual SNPs can also  
176 signify the presence of potential bias from pleiotropy and was assessed using the Cochran's Q test  
177 [43]. All Mendelian randomization analyses were performed using the "MendelianRandomization"  
178 package for R statistical software [44].

179

#### 180 *Colocalisation analysis*

181 For any primary outcomes where there was Mendelian randomization evidence of an effect of  
182 SLC13A5 inhibition, we performed colocalisation analysis using a 200kB window around the SLC13A5  
183 gene, as detailed above [45]. This analysis aims to test whether there is a shared causal variant  
184 underlying any observed Mendelian randomization association, which would support a causal effect  
185 of SLC13A5 inhibition on the outcome [46].

186

#### 187 *Phenome-wide association study*

188 PheWAS was performed in the UK Biobank, a prospective cohort study initiated in 2006 that  
189 recruited more than 500,000 participants aged between 40 and 69 years [47]. Participants  
190 contributed phenotypic and genetic data, as well as biological samples, as previously reported [48].  
191 UK Biobank has approval from the North West Multi-centre Research Ethics Committee and all  
192 participants provided appropriate consent.

193 PheWAS statistical analysis was performed by first constructing a weighted genetic risk score for the  
194 exposure using the same instrument SNPs as employed in the Mendelian randomization analysis. For  
195 each individual included in the analysis, the number of plasma citrate-increasing alleles for each

196 instrument SNP were multiplied by the corresponding genetic association estimate with citrate for  
197 that SNP, before combining by addition. International Classification of Diseases versions 9 and 10  
198 were used to ascertain cases in the UK Biobank Hospital Episode Statistics data, with diagnoses  
199 linked to the phenotype code (phecode) grouping system to facilitate classification of clinically  
200 relevant traits [49]. Logistic regression was performed for each phecode against the standardized  
201 genetic risk score for the exposure, adjusting for age, sex, and the first 10 genetic principal  
202 components of genetic ancestry. Only phecodes with 200 or more cases were included in the  
203 analysis, to avoid inclusion of outcomes with low statistical power. PheWAS estimates are reported  
204 per 1-SD higher standardized exposure genetic risk score. PheWAS was conducted using the  
205 “PheWAS” package of R statistical software [50].

206

#### 207 *Statistical significance ascertainment*

208 To account for testing of multiple outcomes in the primary Mendelian randomization analysis of  
209 renal outcomes, the Benjamini–Hochberg false discovery rate (FDR) 5% threshold was used. No  
210 statistical significance threshold was used for the other analyses, which were exploratory in nature.  
211 All presented p-values are uncorrected for multiple testing, unless otherwise stated.

212

#### 213 *Comparison of SLC13A5 inhibition with higher plasma citrate levels by any mechanism*

214 The Mendelian randomization and PheWAS analyses were also performed considering the exposure  
215 of plasma citrate levels, rather than SLC13A5 inhibition. Selection of genetic variants to serve as  
216 instruments and build the weighted genetic risk score for plasma citrate was undertaken using the  
217 same approach as for SLC13A5 inhibition, except that selection of variants was not confined to the  
218 *SLC13A5* gene region.

219

220 *Availability of code and data*

221 R statistical software was used for all analyses. The statistical code used in this work is available upon  
222 reasonable request to the corresponding author. All genome-wide association study summary data  
223 are publicly available from the sources cited in Table 1. UK Biobank individual participant data are  
224 available upon appropriate application to the UK Biobank study. This work was reported using the  
225 “Strengthening the Reporting of Observational Studies in Epidemiology using Mendelian  
226 Randomization” (STROBE-MR) checklist (Additional file 1) [51].

## 227 Results

228 A total of 13 SNPs were identified as instruments for SLC13A5 inhibition (Additional file 2: Table S1),  
229 all of which had F-statistics > 10, consistent with low risk of weak instrument bias that might affect  
230 the conclusions of Mendelian randomization analyses. Functional annotations of the SNPs obtained  
231 using PhenoScanner version 2 are provided in Additional file 2: Table S2. There were only potential  
232 pleiotropic associations of one variant (rs75448233) with smoking traits, however these associations  
233 did not reach genome-wide significance (Additional file 2: Table S3).

234 The main IVW Mendelian randomization identified positive associations of genetically proxied  
235 SLC13A5 inhibition with plasma calcium levels. Every 1-SD higher genetically proxied plasma citrate  
236 through SLC13A5 inhibition was associated with a 0.132 SD units higher plasma calcium level (95% CI  
237 0.107 to 0.157,  $p=6 \times 10^{-13}$ ).

238 Figure 2 depicts the associations of genetically proxied SLC13A5 inhibition with kidney function  
239 parameters from the main IVW Mendelian randomization analysis. There were statistically significant  
240 associations of genetically proxied SLC13A5 inhibition with higher creatinine and cystatin C based  
241 measures of eGFR (FDR adjusted p values = 0.006 and 0.010 respectively), and lower BUN (FDR  
242 adjusted p value = 0.002). There were no strong associations of genetically proxied SLC13A5  
243 inhibition with uACR (FDR adjusted p value = 0.682), or risk of CKD (FDR adjusted p value = 0.516) or  
244 microalbuminuria (FDR adjusted p value = 0.682). Additional file 3: Fig. S1-S6 show scatter plots of  
245 the SNP-exposure and SNP-outcome associations. Similar Mendelian randomization point estimates  
246 were obtained when using a pruning threshold of  $r^2 < 0.01$  (Additional file 2: Table S4).

247 Results of the colocalisation analysis for primary outcomes showing significant Mendelian  
248 randomization associations are presented in Additional file 2: Table S5. For all these analyses, there  
249 was only evidence of a causal variant in the locus affecting plasma citrate levels, suggesting that  
250 there was inadequate statistical power to test whether the Mendelian randomization associations  
251 were attributable to shared or distinct causal variants [46].

252 The results of the metabolome-wide Mendelian randomization analysis investigating the effects of  
253 SLC13A5 inhibition on plasma and urine metabolites are presented in Additional file 2: Table S6 and  
254 S7. As expected, there was genetic evidence supporting associations of SLC13A5 inhibition with  
255 higher plasma citrate. Additionally, there was evidence supporting associations of SLC13A5 inhibition  
256 with higher plasma aconitate and plasma N-acetylspermidine.

257 The main IVW Mendelian randomization analysis results measuring the association of genetically  
258 proxied SLC13A5 inhibition with parameters of glucose and lipid metabolism, and inflammation are  
259 presented in Figure 3. In this hypothesis-generating analysis, there were no significant associations  
260 after adjusting for multiple testing, but some evidence to support possible associations of SLC13A5  
261 inhibition with lower fasting glucose levels (-0.026 mmol/l per 1-SD higher plasma citrate through  
262 SCL13A5 inhibition, 95% CI -0.047 to 0.004, raw p=0.022) [10,21]. Neither proteome-wide Mendelian  
263 randomization (Additional file 2: Table S8) nor PheWAS (Additional file 2: Table S9) identified any  
264 significant associations for genetically proxied SLC13A5 inhibition after correcting for multiple testing.

265 All analyses were also performed considering higher plasma citrate through any mechanism as the  
266 exposure, instead of genetically proxied SLC13A5 inhibition (i.e., SNPs associated with higher plasma  
267 citrate selected as in the analysis for SLC13A5, but not restricted to 200kB within the *SLC13A5* gene).

268 The SNPs used as instruments for plasma citrate are presented in Additional file 2: Table S10, and the  
269 analysis results are presented in Additional file 2: Tables S11-S14. Although the main IVW analysis did  
270 not identify evidence supporting associations of genetically predicted plasma citrate levels with eGFR  
271 or BUN, the Egger and weighted median sensitivity analyses that are more robust to the inclusion of  
272 pleiotropic SNPs were more supportive of such an association (Additional file 2: Table S15). This  
273 suggests that the genetic variants that affect plasma citrate are heterogeneous and pleiotropic in the  
274 mechanisms by which they achieve effects on eGFR and BUN. Consistent with this, there was strong  
275 evidence of heterogeneity in all the IVW MR analyses undertaken with plasma citrate as the  
276 exposure (Additional file 2: Table S15). This implies that increasing plasma citrate through SLC13A5

- 277 inhibition would potentially improve eGFR and BUN, but that increasing plasma citrate by other  
278 mechanism not necessarily achieve this same result.

## 279 Discussion

280 Using large-scale genetic association data, we identified a genetic instrument for SLC13A5 inhibition  
281 that we leveraged in the Mendelian randomization paradigm to provide clinically translatable  
282 insights. Our main findings generated human genetic evidence that supports higher plasma citrate  
283 and calcium as biologically plausible biomarkers of target engagement, higher plasma citrate as a  
284 potential mechanism of action biomarker, and favourable effects on parameters of kidney function,  
285 namely creatinine and cystatin C based measures of eGFR, and BUN. Of note, we did not identify  
286 statistically significant evidence of effects of SLC13A5 inhibition on uACR nor risk of  
287 microalbuminuria. This discrepancy may be explained by these biomarkers measuring different  
288 domains of kidney function [52]. Of relevance, calcium citrate treatment in an acute kidney damage  
289 animal model resulted in significantly reduced levels of proteinuria [1]. The primary Mendelian  
290 randomization analysis also did not identify evidence of SLC13A5 inhibition having effects on CKD  
291 risk, which may in part be explained by the pathophysiological heterogeneity underlying CKD [53],  
292 and SLC13A5 inhibition potentially only being relevant to some of these mechanisms.

293 Secondary Mendelian randomization analyses supported potential effects of SLC13A5 inhibition on  
294 reducing fasting glucose. Given that SLC13A5 is predominantly expressed in the liver [26], these  
295 findings are consistent with direct hepatic effects. The lack of strong associations of genetically  
296 proxied SLC13A5 inhibition with clinical outcomes in PheWAS is reassuring regarding safety profile,  
297 although the limited statistical power also means that findings may warrant further investigation .  
298 This suggests smaller reductions in SLC13A5 activity are unlikely to recapitulate the autosomal-  
299 recessive epileptic encephalopathy phenotype observed with rare mutations affecting critical regions  
300 of the *SLC13A5* gene [54].

301 SLC13A5 is a membrane-bound citrate transporter, and its inhibition results in reduced entry of  
302 plasma citrate into the cytosol [4,5]. This would be expected to have implications for cellular  
303 metabolism in cells expressing SLC13A5, with the higher circulating plasma citrate levels also



304 potentially impacting metabolism systemically. Consistent with the results of our main genetic  
305 analyses, previous work has identified protective effects of citrate in various animal models of kidney  
306 disease [1,6,55,56]. Although the main IVW Mendelian randomization analysis investigating effects of  
307 plasma citrate levels did not identify evidence supporting effects on parameters of kidney function,  
308 there was strong evidence of heterogeneity in estimates generated by individual SNPs, consistent  
309 with the presence of pleiotropic effects that could bias the main IVW analyses [43]. Furthermore, the  
310 Egger and weighted median Mendelian randomization statistical sensitivity analyses, which can be  
311 more robust to the inclusion of pleiotropic variants, produced estimates more suggestive of  
312 favourable effects of higher plasma citrate on measures of kidney function. This observation may  
313 suggest that plasma citrate is a heterogeneous trait that is affected through several distinct  
314 pathways, and that at least some of these may favourably impact kidney function. This would be in-  
315 keeping with the favourable effects of SLC13A5 on kidney function occurring through its effects on  
316 plasma citrate. It has been reported that low citrate levels in urine are associated with various forms  
317 of kidney disease, and low urinary citrate is a biomarker for kidney disease progression [55,57–62].  
318 Furthermore, preclinical studies with SLC13A5 knockout mice have supported effects on  
319 sympathoadrenal mechanisms [63], which may also contribute to nephroprotective effects of  
320 genetically proxied SLC13A5 inhibition.

321 There are several hypotheses for how citrate may exert its beneficial effects on kidney function.  
322 Generally, elevated plasma citrate levels are proposed to lead to increased excretion of citrate  
323 through the urine. Higher urinary citrate may in turn provide an additional energy supply for kidney  
324 cells [1–3], potentially enhancing their resilience and function. Furthermore, citrate may contribute  
325 to supporting the biosynthesis of essential molecules such as glucose, lipids, and amino acids.  
326 Additionally, it is known, due to its alkalinizing function citrate contributes to improved acid-base  
327 balance within the kidneys, promoting a favourable environment for cellular processes. Finally,  
328 urinary citrate's solubilizing properties might offer protection against vascular calcification and the  
329 formation of kidney stones, thus safeguarding kidney health.

330 This work has several strengths. By leveraging large-scale genetic association data within the  
331 Mendelian randomization paradigm, we were able to rapidly perform several hypothesis-driven and  
332 hypothesis-free genetic analyses relevant to humans, and consequently generate insight related to  
333 drug development. Our findings represent numerous potential learnings, including highlighting  
334 higher plasma citrate and calcium as biomarkers of target engagement, higher plasma citrate as a  
335 biomarker of mechanism of action, efficacy for improving kidney function, general safety profile, and  
336 potential effects on reducing fasting glucose. Further, the random allocation of genetic variants at  
337 conception means that these findings are less vulnerable to the confounding and reverse causation  
338 bias that can hinder causal inference in traditional epidemiological study designs [64].

339 This work should also be interpreted in the context of its limitations. The Mendelian randomization  
340 paradigm considers small lifelong effects of germline genetic variation. This is not the same as a  
341 discrete clinical intervention in later life, which may be of shorter duration but larger magnitude.  
342 Thus, it is possible that some of the findings of these genetic analyses may not predict what is  
343 observed with inhibition of SLC13A5 in clinical practice, particularly in quantitative terms. Further,  
344 some of our current analyses may also be limited by phenotypic definition and statistical power. For  
345 example, we note that kidney traits were not prioritised in the results of PheWAS analysis. In  
346 addition, the colocalization analyses did not support a single causal variant underlying the observed  
347 Mendelian randomization associations, and this may be attributable to either low statistical power,  
348 or confounding due to variant in linkage disequilibrium. In the Mendelian randomization analyses,  
349 we used a combination of European ancestry and multi-ancestry genetic association data, creating  
350 the potential for bias related to population substructure. Similarly, there may be interactions of the  
351 genetic variants employed as instruments with dietary intake of citrate, which may vary across  
352 population groups, potentially also introducing bias. While challenges in estimating the variance of  
353 drug target perturbation predicted by genetic variants means that it is not possible to perform  
354 conventional power calculations for drug target Mendelian randomization [65], some indication of  
355 the relative statistical power available for each analysis is apparent from the size of the 95% CIs.

356 From this, it is clear that the analyses considering CKD had much less power than those considering  
357 measures of eGFR or BUN, for example. Of relevance, numerous preclinical mechanistic studies have  
358 demonstrated a role of SLC13A5 in favourably affecting hepatic lipid and glucose metabolism [10–  
359 13,20,21,66,67], and the limitations of our current analyses may explain the discrepancy in findings.  
360 The plasma and urine metabolome-wide Mendelian randomization analyses were undertaken using  
361 outcome data obtained from a CKD population and may thus be vulnerable to collider bias [68]. This  
362 is because stratifying on a collider can introduce associations with confounding factors. Our  
363 Mendelian randomization evidence supports effects of SLC13A5 inhibition on parameters of kidney  
364 function, in-keeping with CKD therefore representing a potential collider. While there are strategies  
365 available to help explore potential bias from this [69], they either require individual participant data,  
366 which were not available for the current Mendelian randomization analyses, or have other  
367 prohibitive limitations [70]. Finally, the genetic analyses undertaken in this work provide insight into  
368 the on-target effects of perturbing SLC13A5 [19], but cannot directly inform on the effects of any  
369 pharmacological agents used to inhibit SLC13A5, including their pharmacokinetic and  
370 pharmacodynamic properties, or off-target effects.

371

## 372 **Conclusions**

373 In summary, this Mendelian randomization analysis provides novel human-centric insight to guide  
374 the clinical development of an SLC13A5 inhibitor. We identify biologically plausible biomarkers of  
375 target engagement and mode of action, as well as genetic evidence supporting potential effects in  
376 improving kidney function, with higher plasma citrate levels a possible underlying mechanism. The  
377 null PheWAS findings are reassuring in that they do not identify any safety signals. Further study in  
378 the form of early-stage clinical trials may now be warranted to help translate these findings towards  
379 improving patient care.

380 **Acronyms**

381 BUN: blood urea nitrogen

382 CI: confidence interval

383 CKD: chronic kidney disease

384 CRP: c-reactive protein

385 eGFR: estimated glomerular filtration rate

386 FDR: false-discovery rate

387 GWAS: genome-wide association study

388 HDLc: high-density lipoprotein cholesterol

389 IL6: interleukin-6

390 IVW: inverse-variance weighted

391 LDLc: low-density lipoprotein cholesterol

392 OR: odds ratio

393 PheWAS: phenome-wide association study

394 SD: standard deviation

395 SNP: single-nucleotide polymorphism

396 uACR: urine albumin-creatinine ratio

397 **Declarations**

398 ***Authors' Twitter handles***

399 @dpsg108

400 @LoukasZagkos

401 @RubinderGill

402 @stevesphd

403

404 ***Acknowledgements***

405 The authors thank all the studies and participants contributing the data used in this work.

406

407 ***Consent for Publication***

408 No identifiable individual participant data were used in this study. All studies contributing genetic  
409 association summary data obtained appropriate participant consent and ethical approvals in the  
410 original studies, including for publication. All authors have approved the final submission of this  
411 article for publication.

412

413 ***Funding***

414 This work was supported by Eternygen GmbH. Dipender Gill acknowledges support by the British  
415 Heart Foundation Centre of Research Excellence at Imperial College London (RE/18/4/34215).  
416 Stephen Burgess is supported by the Wellcome Trust (225790/Z/22/Z) and the United Kingdom  
417 Research and Innovation Medical Research Council (MC\_UU\_00002/7).

418

419 ***Availability of Data and Materials***

420 R statistical software was used for all analyses. The statistical code used in this work is available upon  
421 reasonable request to the corresponding author. All genome-wide association study summary data  
422 are publicly available from the sources cited in Table 1. UK Biobank individual participant data are  
423 available upon appropriate application to the UK Biobank study.

424

425 ***Authors' Contributions***

426 DG and GZ conceived the study design. DG and LZ performed statistical analysis. DG drafted the  
427 manuscript. LZ, RG, TB, JJ, ALB, SB and GZ edited the manuscript for intellectual content. All authors  
428 read and approved the final manuscript.

429

430 ***Competing interests***

431 DG and RG are employed part-time by Primula Group. SB has received personal fees from Primula  
432 Group. ALB and JJ are minor shareholders of Eternygen GmbH, and GZ is minor shareholder and  
433 employee of Eternygen GmbH. ALB has received research funding from Boehringer Ingelheim und  
434 AstraZeneca.

435

436 ***Ethics Approval and Consent to Participate***

437 The genome-wide association study summary data sources used for the Mendelian randomization  
438 analyses are presented in Table 1, and the data are publicly available from the cited sources.  
439 Participant consent and ethical approval for all data were obtained in the original studies.

440 **References**

- 441 [1] Gadola L, Noboa O, Marquez MN, Rodriguez MJ, Nin N, Boggia J, et al. Calcium citrate  
442 ameliorates the progression of chronic renal injury. *Kidney Int* 2004;65.  
443 <https://doi.org/10.1111/j.1523-1755.2004.00496.x>.
- 444 [2] Weinberg JM, Venkatachalam MA, Roeser NF, Saikumar P, Dong Z, Senter RA, et al.  
445 Anaerobic and aerobic pathways for salvage of proximal tubules from hypoxia-induced  
446 mitochondrial injury. *Am J Physiol Renal Physiol* 2000;279.  
447 <https://doi.org/10.1152/ajprenal.2000.279.5.f927>.
- 448 [3] Feldkamp T, Kribben A, Roeser NF, Senter RA, Weinberg JM. Accumulation of  
449 nonesterified fatty acids causes the sustained energetic deficit in kidney proximal  
450 tubules after hypoxia-reoxygenation. *Am J Physiol Renal Physiol* 2006;290.  
451 <https://doi.org/10.1152/ajprenal.00305.2005>.
- 452 [4] Zhang L, Hu W, Qiu Z, Li Z, Bian J. Opportunities and Challenges for Inhibitors Targeting  
453 Citrate Transport and Metabolism in Drug Discovery. *J Med Chem* 2023.  
454 <https://doi.org/10.1021/acs.jmedchem.3c00179>.
- 455 [5] Inoue K, Zhuang L, Maddox DM, Smith SB, Ganapathy V. Human sodium-coupled  
456 citrate transporter, the orthologue of *Drosophila* Indy, as a novel target for lithium  
457 action. *Biochemical Journal* 2003;374. <https://doi.org/10.1042/BJ20030827>.
- 458 [6] Bienholz A, Reis J, Sanli P, De Groot H, Petrat F, Guberina H, et al. Citrate shows  
459 protective effects on cardiovascular and renal function in ischemia-induced acute  
460 kidney injury. *BMC Nephrol* 2017;18. <https://doi.org/10.1186/s12882-017-0546-1>.
- 461 [7] Akhtar MJ, Khan SA, Kumar B, Chawla P, Bhatia R, Singh K. Role of sodium dependent  
462 SLC13 transporter inhibitors in various metabolic disorders. *Mol Cell Biochem*  
463 2023;478. <https://doi.org/10.1007/s11010-022-04618-7>.

- 464 [8] Willmes DM, Kurzbach A, Henke C, Schumann T, Zahn G, Heifetz A, et al. The longevity  
465 gene INDY (I'm Not Dead Yet) in metabolic control: Potential as pharmacological  
466 target. *Pharmacol Ther* 2018;185. <https://doi.org/10.1016/j.pharmthera.2017.10.003>.
- 467 [9] Schumann T, König J, Henke C, Willmes DM, Bornstein SR, Jordan J, et al. Solute carrier  
468 transporters as potential targets for the treatment of metabolic disease. *Pharmacol*  
469 *Rev* 2020;72. <https://doi.org/10.1124/pr.118.015735>.
- 470 [10] Birkenfeld AL, Lee HY, Guebre-Egziabher F, Alves TC, Jurczak MJ, Jornayvaz FR, et al.  
471 Deletion of the mammalian INDY homolog mimics aspects of dietary restriction and  
472 protects against adiposity and insulin resistance in mice. *Cell Metab* 2011;14.  
473 <https://doi.org/10.1016/j.cmet.2011.06.009>.
- 474 [11] von Loeffelholz C, Lieske S, Neuschäfer-Rube F, Willmes DM, Raschzok N, Sauer IM, et  
475 al. The human longevity gene homolog INDY and interleukin-6 interact in hepatic lipid  
476 metabolism. *Hepatology* 2017;66. <https://doi.org/10.1002/hep.29089>.
- 477 [12] Zahn G, Willmes DM, El-Agroudy NN, Yarnold C, Jarjes-Pike R, Schaertl S, et al. A Novel  
478 and Cross-Species Active Mammalian INDY (NaCT) Inhibitor Ameliorates Hepatic  
479 Steatosis in Mice with Diet-Induced Obesity. *Metabolites* 2022;12.  
480 <https://doi.org/10.3390/metabo12080732>.
- 481 [13] Huard K, Brown J, Jones JC, Cabral S, Futatsugi K, Gorgoglione M, et al. Discovery and  
482 characterization of novel inhibitors of the sodium-coupled citrate transporter (NaCT or  
483 SLC13A5). *Sci Rep* 2015;5. <https://doi.org/10.1038/srep17391>.
- 484 [14] Kopel JJ, Bhutia YD, Sivaprakasam S, Ganapathy V. Consequences of  
485 NaCT/SLC13A5/mINDY deficiency: Good versus evil, separated only by the blood-brain  
486 barrier. *Biochemical Journal* 2021;478. <https://doi.org/10.1042/BCJ20200877>.



- 487 [15] Gopal E, Babu E, Ramachandran S, Bhutia YD, Prasad PD, Ganapathy V. Species-specific  
488 influence of lithium on the activity of SLC13A5 (NACT): Lithium-induced activation is  
489 specific for the transporter in primates. *Journal of Pharmacology and Experimental*  
490 *Therapeutics* 2015;353. <https://doi.org/10.1124/jpet.114.221523>.
- 491 [16] Inoue K, Zhuang L, Ganapathy V. Human Na<sup>+</sup>-coupled citrate transporter: Primary  
492 structure, genomic organization, and transport function. *Biochem Biophys Res*  
493 *Commun* 2002;299. [https://doi.org/10.1016/S0006-291X\(02\)02669-4](https://doi.org/10.1016/S0006-291X(02)02669-4).
- 494 [17] Hingorani AD, Kuan V, Finan C, Kruger FA, Gaulton A, Chopade S, et al. Improving the  
495 odds of drug development success through human genomics: modelling study. *Sci Rep*  
496 2019;9. <https://doi.org/10.1038/s41598-019-54849-w>.
- 497 [18] Gill D, Georgakis MK, Walker VM, Schmidt AF, Gkatzionis A, Freitag DF, et al. Mendelian  
498 randomization for studying the effects of perturbing drug targets. *Wellcome Open Res*  
499 2021;6. <https://doi.org/10.12688/wellcomeopenres.16544.2>.
- 500 [19] Burgess S, Mason AM, Grant AJ, Slob EAW, Gkatzionis A, Zuber V, et al. Using genetic  
501 association data to guide drug discovery and development: Review of methods and  
502 applications. *Am J Hum Genet* 2023;110. <https://doi.org/10.1016/j.ajhg.2022.12.017>.
- 503 [20] Pesta DH, Perry RJ, Guebre-Egziabher F, Zhang D, Jurczak M, Fischer-Rosinsky A, et al.  
504 Prevention of diet-induced hepatic steatosis and hepatic insulin resistance by second  
505 generation antisense oligonucleotides targeted to the longevity gene mIndy (Slc13a5).  
506 *Aging* 2015;7. <https://doi.org/10.18632/aging.100854>.
- 507 [21] Brachs S, Winkel AF, Tang H, Birkenfeld AL, Brunner B, Jahn-Hofmann K, et al. Inhibition  
508 of citrate cotransporter Slc13a5/mINDY by RNAi improves hepatic insulin sensitivity  
509 and prevents diet-induced non-alcoholic fatty liver disease in mice. *Mol Metab* 2016;5.  
510 <https://doi.org/10.1016/j.molmet.2016.08.004>.

- 511 [22] Brown TL, Nye KL, Porter BE. Growth and overall health of patients with slc13a5 citrate  
512 transporter disorder. *Metabolites* 2021;11. <https://doi.org/10.3390/metabo11110746>.
- 513 [23] Bainbridge MN, Cooney E, Miller M, Kennedy AD, Wulff JE, Donti T, et al. Analyses of  
514 SLC13A5-epilepsy patients reveal perturbations of TCA cycle. *Mol Genet Metab*  
515 2017;121. <https://doi.org/10.1016/j.ymgme.2017.06.009>.
- 516 [24] Costello LC, Franklin RB. Plasma Citrate Homeostasis: How It Is Regulated; And Its  
517 Physiological and Clinical Implications. An Important, But Neglected, Relationship in  
518 Medicine. *HSOA J Hum Endocrinol* 2016;1.
- 519 [25] Kamat MA, Blackshaw JA, Young R, Surendran P, Burgess S, Danesh J, et al.  
520 PhenoScanner V2: An expanded tool for searching human genotype-phenotype  
521 associations. *Bioinformatics* 2019;35. <https://doi.org/10.1093/bioinformatics/btz469>.
- 522 [26] Li Z, Wang H. Molecular mechanisms of the SLC13A5 gene transcription. *Metabolites*  
523 2021;11. <https://doi.org/10.3390/metabo111100706>.
- 524 [27] Denny JC, Ritchie MD, Basford MA, Pulley JM, Bastarache L, Brown-Gentry K, et al.  
525 PheWAS: Demonstrating the feasibility of a phenome-wide scan to discover gene-  
526 disease associations. *Bioinformatics* 2010;26.  
527 <https://doi.org/10.1093/bioinformatics/btq126>.
- 528 [28] Li B, Martin EB. An approximation to the F distribution using the chi-square  
529 distribution. *Comput Stat Data Anal* 2002;40. [https://doi.org/10.1016/S0167-](https://doi.org/10.1016/S0167-9473(01)00097-4)  
530 [9473\(01\)00097-4](https://doi.org/10.1016/S0167-9473(01)00097-4).
- 531 [29] Elsworth B, Lyon M, Alexander T, Liu Y, Matthews P, Hallett J, et al. The MRC IEU  
532 OpenGWAS data infrastructure. *BioRxiv* 2020.
- 533 [30] Neale Lab. GWAS of UK Biobank biomarker measurements 2023.

- 534 [31] Stanzick KJ, Li Y, Schlosser P, Gorski M, Wuttke M, Thomas LF, et al. Discovery and  
535 prioritization of variants and genes for kidney function in >1.2 million individuals. *Nat*  
536 *Commun* 2021;12. <https://doi.org/10.1038/s41467-021-24491-0>.
- 537 [32] Teumer A, Li Y, Ghasemi S, Prins BP, Wuttke M, Hermle T, et al. Genome-wide  
538 association meta-analyses and fine-mapping elucidate pathways influencing  
539 albuminuria. *Nat Commun* 2019;10. <https://doi.org/10.1038/s41467-019-11576-0>.
- 540 [33] Wuttke M, Li Y, Li M, Sieber KB, Feitosa MF, Gorski M, et al. A catalog of genetic loci  
541 associated with kidney function from analyses of a million individuals. *Nat Genet*  
542 2019;51. <https://doi.org/10.1038/s41588-019-0407-x>.
- 543 [34] Schlosser P, Scherer N, Grundner-Culemann F, Monteiro-Martins S, Haug S,  
544 Steinbrenner I, et al. Genetic studies of paired metabolomes reveal enzymatic and  
545 transport processes at the interface of plasma and urine. *Nat Genet* 2023;55.  
546 <https://doi.org/10.1038/s41588-023-01409-8>.
- 547 [35] Graham SE, Clarke SL, Wu KHH, Kanoni S, Zajac GJM, Ramdas S, et al. The power of  
548 genetic diversity in genome-wide association studies of lipids. *Nature* 2021;600.  
549 <https://doi.org/10.1038/s41586-021-04064-3>.
- 550 [36] Chen J, Spracklen CN, Marenne G, Varshney A, Corbin LJ, Luan J, et al. The trans-  
551 ancestral genomic architecture of glycemetic traits. *Nat Genet* 2021;53.  
552 <https://doi.org/10.1038/s41588-021-00852-9>.
- 553 [37] Haas ME, Pirruccello JP, Friedman SN, Wang M, Emdin CA, Ajmera VH, et al. Machine  
554 learning enables new insights into genetic contributions to liver fat accumulation. *Cell*  
555 *Genomics* 2021;1. <https://doi.org/10.1016/j.xgen.2021.100066>.

- 556 [38] Ferkingstad E, Sulem P, Atlason BA, Sveinbjornsson G, Magnusson MI, Styrismisdottir EL,  
557 et al. Large-scale integration of the plasma proteome with genetics and disease. *Nat*  
558 *Genet* 2021;53. <https://doi.org/10.1038/s41588-021-00978-w>.
- 559 [39] Said S, Pazoki R, Karhunen V, Vösa U, Ligthart S, Bodinier B, et al. Genetic analysis of  
560 over half a million people characterises C-reactive protein loci. *Nat Commun* 2022;13.  
561 <https://doi.org/10.1038/s41467-022-29650-5>.
- 562 [40] Burgess S, Butterworth A, Thompson SG. Mendelian randomization analysis with  
563 multiple genetic variants using summarized data. *Genet Epidemiol* 2013;37:658–65.  
564 <https://doi.org/10.1002/gepi.21758>.
- 565 [41] Bowden J, Davey Smith G, Burgess S. Mendelian randomization with invalid  
566 instruments: effect estimation and bias detection through Egger regression. *Int J*  
567 *Epidemiol* 2015;44:512–25. <https://doi.org/10.1093/ije/dyv080>.
- 568 [42] Bowden J, Davey Smith G, Haycock PC, Burgess S. Consistent Estimation in Mendelian  
569 Randomization with Some Invalid Instruments Using a Weighted Median Estimator.  
570 *Genet Epidemiol* 2016;40:304–14. <https://doi.org/10.1002/gepi.21965>.
- 571 [43] Greco M F Del, Minelli C, Sheehan NA, Thompson JR. Detecting pleiotropy in  
572 Mendelian randomisation studies with summary data and a continuous outcome. *Stat*  
573 *Med* 2015;34. <https://doi.org/10.1002/sim.6522>.
- 574 [44] Yavorska OO, Burgess S. MendelianRandomization: An R package for performing  
575 Mendelian randomization analyses using summarized data. *Int J Epidemiol* 2017;46.  
576 <https://doi.org/10.1093/ije/dyx034>.
- 577 [45] Giambartolomei C, Vukcevic D, Schadt EE, Franke L, Hingorani AD, Wallace C, et al.  
578 Bayesian Test for Colocalisation between Pairs of Genetic Association Studies Using

579 Summary Statistics. *PLoS Genet* 2014;10.  
580 <https://doi.org/10.1371/journal.pgen.1004383>.

581 [46] Zuber V, Grinberg NF, Gill D, Manipur I, Slob EAW, Patel A, et al. Combining evidence  
582 from Mendelian randomization and colocalization: Review and comparison of  
583 approaches. *Am J Hum Genet* 2022;109. <https://doi.org/10.1016/j.ajhg.2022.04.001>.

584 [47] Sudlow C, Gallacher J, Allen N, Beral V, Burton P, Danesh J, et al. UK Biobank: An Open  
585 Access Resource for Identifying the Causes of a Wide Range of Complex Diseases of  
586 Middle and Old Age. *PLoS Med* 2015;12.  
587 <https://doi.org/10.1371/journal.pmed.1001779>.

588 [48] Bycroft C, Freeman C, Petkova D, Band G, Elliott LT, Sharp K, et al. The UK Biobank  
589 resource with deep phenotyping and genomic data. *Nature* 2018;562.  
590 <https://doi.org/10.1038/s41586-018-0579-z>.

591 [49] Wu P, Gifford A, Meng X, Li X, Campbell H, Varley T, et al. Mapping ICD-10 and ICD-10-  
592 CM Codes to phecodes: Workflow development and initial evaluation. *JMIR Med  
593 Inform* 2019;7. <https://doi.org/10.2196/14325>.

594 [50] Carroll RJ, Bastarache L, Denny JC. R PheWAS: Data analysis and plotting tools for  
595 phenome-wide association studies in the R environment. *Bioinformatics* 2014;30.  
596 <https://doi.org/10.1093/bioinformatics/btu197>.

597 [51] Skrivankova VW, Richmond RC, Woolf BAR, Yarmolinsky J, Davies NM, Swanson SA, et  
598 al. Strengthening the Reporting of Observational Studies in Epidemiology Using  
599 Mendelian Randomization: The STROBE-MR Statement. *JAMA - Journal of the  
600 American Medical Association* 2021;326. <https://doi.org/10.1001/jama.2021.18236>.

601 [52] Lopez-Giacoman S. Biomarkers in chronic kidney disease, from kidney function to  
602 kidney damage. *World J Nephrol* 2015;4. <https://doi.org/10.5527/wjn.v4.i1.57>.

- 603 [53] Matovinović MS. 1. Pathophysiology and Classification of Kidney Diseases. EJIFCC  
604 2009;20.
- 605 [54] Thevenon J, Milh M, Feillet F, St-Onge J, Duffourd Y, Jugé C, et al. Mutations in SLC13A5  
606 cause autosomal-recessive epileptic encephalopathy with seizure onset in the first  
607 days of Life. Am J Hum Genet 2014;95. <https://doi.org/10.1016/j.ajhg.2014.06.006>.
- 608 [55] Rocha DR, Xue L, Gomes Sousa HM, Carvalho Matos AC, Hoorn EJ, Salih M, et al.  
609 Urinary Citrate Is Associated with Kidney Outcomes in Early Polycystic Kidney Disease.  
610 Kidney360 2022;3. <https://doi.org/10.34067/KID.0004772022>.
- 611 [56] Tanner GA, Tanner JA. Citrate therapy for polycystic kidney disease in rats. Kidney Int  
612 2000;58. <https://doi.org/10.1111/j.1523-1755.2000.00357.x>.
- 613 [57] Posada-Ayala M, Zubiri I, Martin-Lorenzo M, Sanz-Maroto A, Molero D, Gonzalez-  
614 Calero L, et al. Identification of a urine metabolomic signature in patients with  
615 advanced-stage chronic kidney disease. Kidney Int 2014;85.  
616 <https://doi.org/10.1038/ki.2013.328>.
- 617 [58] Hallan S, Afkarian M, Zelnick LR, Kestenbaum B, Sharma S, Saito R, et al. Metabolomics  
618 and Gene Expression Analysis Reveal Down-regulation of the Citric Acid (TCA) Cycle in  
619 Non-diabetic CKD Patients. EBioMedicine 2017;26.  
620 <https://doi.org/10.1016/j.ebiom.2017.10.027>.
- 621 [59] Liu JJ, Liu S, Gurung RL, Ching J, Kovalik JP, Tan TY, et al. Urine tricarboxylic acid cycle  
622 metabolites predict progressive chronic kidney disease in type 2 diabetes. Journal of  
623 Clinical Endocrinology and Metabolism 2018;103. <https://doi.org/10.1210/jc.2018-00947>.
- 624
- 625 [60] Goraya N, Simoni J, Sager LN, Mamun A, Madias NE, Wesson DE. Urine citrate  
626 excretion identifies changes in acid retention as eGFR declines in patients with chronic

- 627 kidney disease. *Am J Physiol Renal Physiol* 2019;317.  
628 <https://doi.org/10.1152/ajprenal.00044.2019>.
- 629 [61] Mutter S, Valo E, Aittomäki V, Nybo K, Raivonen L, Thorn LM, et al. Urinary metabolite  
630 profiling and risk of progression of diabetic nephropathy in 2670 individuals with type  
631 1 diabetes. *Diabetologia* 2022;65. <https://doi.org/10.1007/s00125-021-05584-3>.
- 632 [62] Domrongkitchaiporn S, Stitchantrakul W, Kochakarn W. Causes of Hypocitraturia in  
633 Recurrent Calcium Stone Formers: Focusing on Urinary Potassium Excretion. *American*  
634 *Journal of Kidney Diseases* 2006;48. <https://doi.org/10.1053/j.ajkd.2006.06.008>.
- 635 [63] Willmes DM, Daniels M, Kurzbach A, Lieske S, Bechmann N, Schumann T, et al. The  
636 longevity gene mIndy (I'm Not Dead, Yet) affects blood pressure through  
637 sympathoadrenal mechanisms. *JCI Insight* 2021;6.  
638 <https://doi.org/10.1172/jci.insight.136083>.
- 639 [64] Burgess S, Butterworth A, Malarstig A, Thompson SG. Use of Mendelian randomisation  
640 to assess potential benefit of clinical intervention. *BMJ* 2012;345.  
641 <https://doi.org/10.1136/bmj.e7325>.
- 642 [65] Burgess S. Sample size and power calculations in Mendelian randomization with a  
643 single instrumental variable and a binary outcome. *Int J Epidemiol* 2014;43.  
644 <https://doi.org/10.1093/ije/dyu005>.
- 645 [66] Neuschäfer-Rube F, Schraplau A, Schewe B, Lieske S, Krützfeldt JM, Ringel S, et al.  
646 Arylhydrocarbon receptor-dependent mIndy (Slc13a5) induction as possible  
647 contributor to benzo[a]pyrene-induced lipid accumulation in hepatocytes. *Toxicology*  
648 2015;337. <https://doi.org/10.1016/j.tox.2015.08.007>.

- 649 [67] Li L, Li H, Garzel B, Yang H, Sueyoshi T, Li Q, et al. SLC13A5 Is a novel transcriptional  
650 target of the pregnane x receptor and sensitizes drug-induced steatosis in human liver.  
651 Mol Pharmacol 2015;87. <https://doi.org/10.1124/mol.114.097287>.
- 652 [68] Paternoster L, Tilling K, Davey Smith G. Genetic epidemiology and Mendelian  
653 randomization for informing disease therapeutics: Conceptual and methodological  
654 challenges. PLoS Genet 2017;13. <https://doi.org/10.1371/journal.pgen.1006944>.
- 655 [69] Mitchell RE, Hartley AE, Walker VM, Gkatzionis A, Yarmolinsky J, Bell JA, et al.  
656 Strategies to investigate and mitigate collider bias in genetic and Mendelian  
657 randomisation studies of disease progression. PLoS Genet 2023;19.  
658 <https://doi.org/10.1371/journal.pgen.1010596>.
- 659 [70] Cai S, Allen RJ, Wain L V, Dudbridge F. Reassessing the association of MUC5B with  
660 survival in idiopathic pulmonary fibrosis. Ann Hum Genet 2023;87:248–53.  
661 <https://doi.org/https://doi.org/10.1111/ahg.12522>.
- 662



663 **Table and Figures**

664 Table 1. Genome-wide association study summary data used for the Mendelian randomization analyses.

Category	Trait	Unit	Population and measure	Sample size	Citation
<b>Biomarker</b>	Plasma citrate	SD	European ancestry UK Biobank participants, using cross-sectional measurements	115,064	[29]
	Plasma calcium	SD	British ancestry UK Biobank participants, using cross-sectional measurements	361,194	[30]
<b>Renal</b>	Creatinine-eGFR	SD of log	Multi-ancestry GWAS meta-analysis, using cross-sectional measurements and formulae as described in the original study	1,201,929	[31]
	Cystatin C-eGFR	SD of log			
	Blood urea nitrogen	SD of log			
	Urine albumin-creatinine ratio	SD of log	Multi-ancestry GWAS meta-analysis, using spot measurements in a population including 51,541 individuals with diabetes	564,257	[32]
	Chronic kidney disease	Log OR	Multi-ancestry GWAS meta-analysis, with case definitions as those with cross-sectional eGFR measurements < 60mL/min/1.73m <sup>2</sup>	625,219 (64,164 cases)	[33]
	Microalbuminuria	Log OR	Multi-ancestry GWAS meta-analysis, defined as urine albumin-creatinine ratio > 30mg/g in spot measurements	348,954 (51,861 cases)	[32]
<b>Metabolome</b>	1,296 plasma metabolites	SD	German Chronic Kidney Disease study, using cross-sectional measurements in individuals with eGFR 30-60ml/min/1.73m <sup>2</sup> , or eGFR >60 ml/min/1.73m <sup>2</sup> with urine albumin-creatinine ratio > 300mg/per g, or urinary protein/creatinine ratio > 500mg/g	5,023	[34]
	1,399 urine metabolites	SD			
<b>Lipid, glucose and inflammation</b>	Plasma low-density lipoprotein cholesterol	SD	European ancestry GWAS meta-analysis, using cross-sectional measurements	1,320,016	[35]
	Plasma high-density lipoprotein cholesterol	SD			
	Plasma triglycerides	SD			
	Fasting plasma glucose	mmol/l	European ancestry GWAS meta-analysis, using cross-sectional measurements	200.622	[36]
	Imaging-derived liver fat (MRI-PDF)	SD	UK Biobank participants, using cross-sectional measurements	36,703	[37]

	Plasma interleukin 6 binding aptamer level	SD	deCODE Icelandic study, using cross-sectional measurements	35,559	[38]
	Plasma C-reactive protein level	SD of log	European ancestry GWAS, using cross-sectional measurements	427,367	[39]
<b>Proteome</b>	4,907 plasma protein-binding aptamers	SD	deCODE Icelandic study, using cross-sectional measurements	35,559	[38]

665 The full list of analysed metabolites and protein-binding aptamers are available in Additional file 2. Full study details and access to GWAS summary data are provided in the  
666 original publications. Exclusions were not made for individuals with polycystic kidney disease or renal stone disease. BUN: blood urea nitrogen; eGFR: estimated glomerular  
667 filtration rate; GWAS: genome-wide association study; MRI-PDFF: magnetic resonance imaging derived proton density fat fraction; OR: odds ratio; SD: standard deviation;  
668 uACR: urine albumin-creatinine ratio.

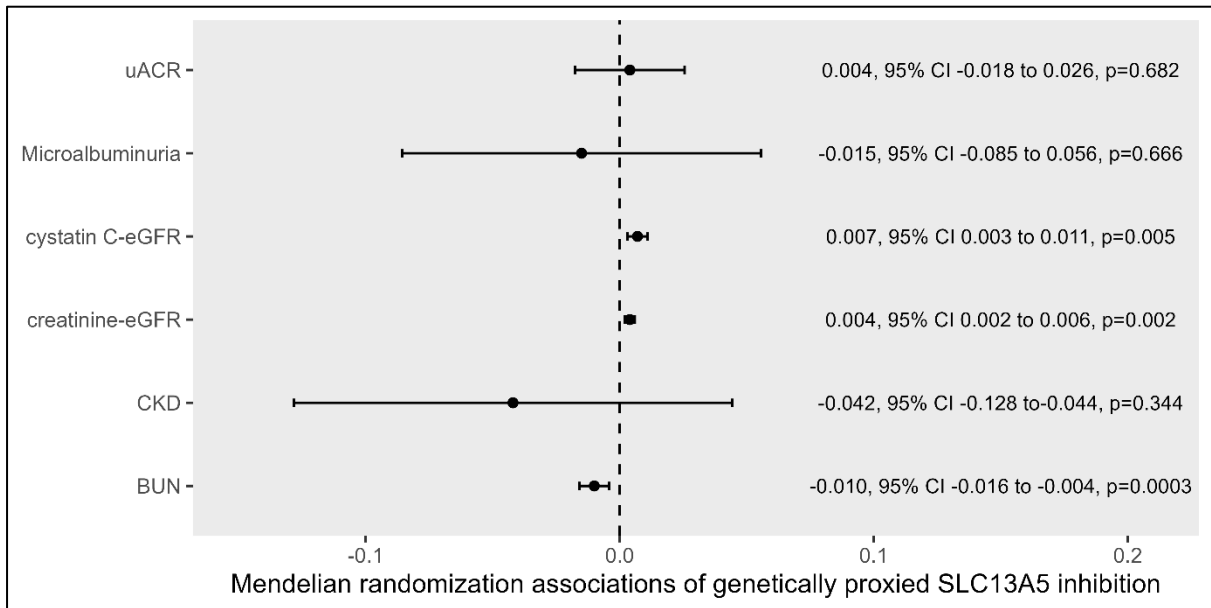
669 Figure 1. Overview of the study design.

	<b>SLC13A5 inhibition</b> Identify genetic instruments for SLC13A5 inhibition <small>SNPs within 200kb of the SLC13A5 gene, uncorrelated (<math>r^2 &lt; 0.1</math>) and associated with plasma citrate at <math>p &lt; 5 \times 10^{-8}</math></small>	<b>Higher plasma citrate</b> Identify genetic instruments for plasma citrate <small>SNPs from throughout the genome, uncorrelated (<math>r^2 &lt; 0.1</math>) and associated with plasma citrate at <math>p &lt; 5 \times 10^{-8}</math></small>	<b>Mendelian randomization sensitivity analyses</b>
	Confirm instrument validity by performing Mendelian randomization to investigate effects on plasma calcium		
Primary analysis	Hypothesis-driven Mendelian randomization analysis investigating effects on parameters of renal function <small>Creatinine-eGFR, cystatin C-eGFR, BUN, uACR, risk of CKD and microalbuminuria</small>		
Exploratory analyses	Exploratory Mendelian randomization analyses investigating effects of SLC13A5 inhibition on: <ol style="list-style-type: none"> <li>1. Plasma and urine metabolites <small>1,296 plasma metabolites and 1,399 urine metabolites</small></li> <li>2. Biomarkers of glucose and lipid metabolism, and inflammation <small>Glucose, HDLc, LDLc and triglycerides, liver fat, IL6, CRP</small></li> <li>3. Plasma proteins <small>4,907 plasma protein-binding aptamers</small></li> </ol> Phenome-wide association study <small>988 clinical outcomes</small>	Repeat all analyses, but considering plasma citrate as the exposure, instead of SLC13A5 inhibition	Egger and weighted median statistical sensitivity analyses

670

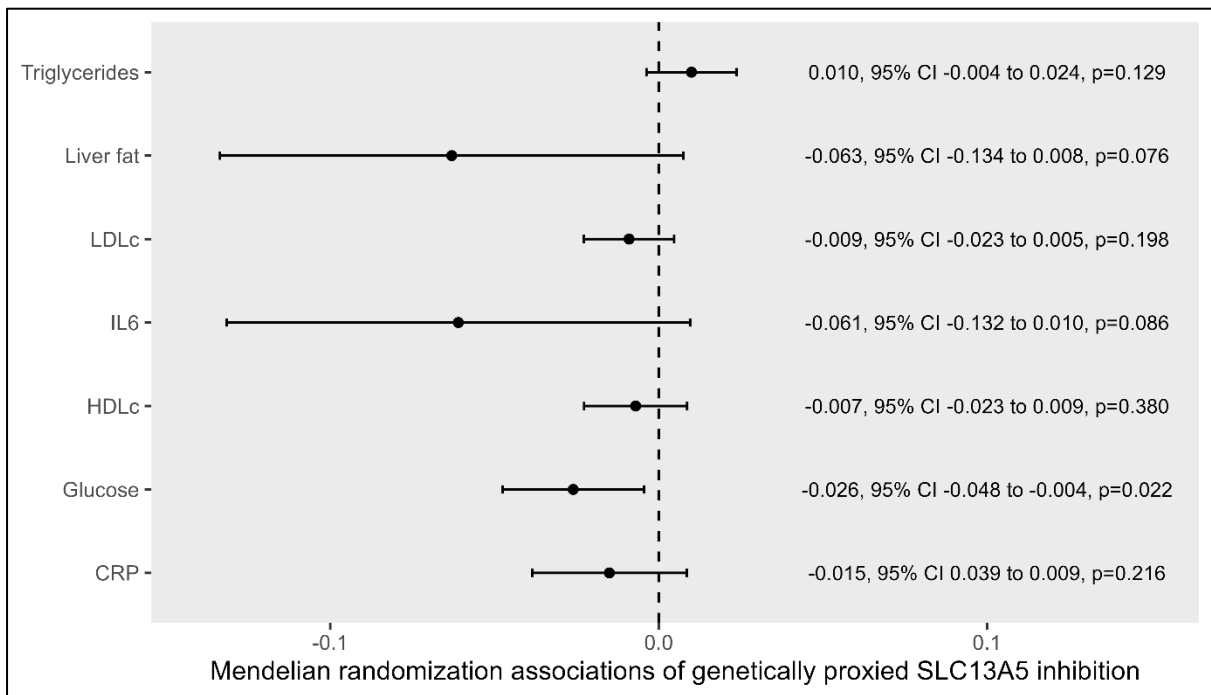
671 BUN: blood urea nitrogen, CRP:C-reactive protein, CKD: chronic kidney disease; eGFR: estimated glomerular  
 672 filtration rate, HDLc: high-density lipoprotein cholesterol, IL6: interleukin 6; LDLc: low-density lipoprotein  
 673 cholesterol, SNP: single-nucleotide polymorphism, uACR: urine albumin-creatinine ratio.

674 Figure 2. Mendelian randomization estimates for the association of genetically proxied SLC13A5  
 675 inhibition with kidney traits.



676  
 677 Mendelian randomization estimates are scaled per 1-standard deviation (SD) increase in plasma citrate through  
 678 genetically proxied SLC13A5 inhibition. The units for the BUN, creatinine-eGFR, cystatin C-eGFR and uACR are  
 679 SD change in log transformed levels. The units for CKD and microalbuminuria are log odds ratio. Raw p values  
 680 are presented. BUN: blood urea nitrogen, chronic kidney disease; eGFR: estimated glomerular filtration rate,  
 681 urine albumin-creatinine ratio.

682 Figure 3. Mendelian randomization estimates for the association of genetically proxied SLC13A5  
 683 inhibition with biomarkers of glucose and lipid metabolism, and inflammation.



684

685 Mendelian randomization estimates are scaled per 1-standard deviation (SD) increase in plasma citrate through  
 686 genetically proxied SLC13A5 inhibition. The units for fasting glucose is mmol/l, the units for C-reactive protein  
 687 (CRP) is standard deviation (SD) change of log transformed levels, and the remaining exposures are measured  
 688 in SD units. HDLc: high-density lipoprotein cholesterol, IL6: interleukin 6, LDLc: low-density lipoprotein  
 689 cholesterol.

690

691 **Additional files**

692 Additional file 1. Strengthening the Reporting of Observational Studies in Epidemiology using  
693 Mendelian Randomization checklist.

694

695 Additional file 2. Tables S1-S15.

696 Table S1. Single-nucleotide polymorphisms used as instruments for SLC13A5 inhibition. Genetic  
697 associations with plasma citrate are presented for variants within 200kB of the *SLC13A5* gene. SNP:  
698 single-nucleotide polymorphism.

699 Table S2. Annotation of the functional consequences of the single-nucleotide polymorphisms used to  
700 instruments SLC13A5 inhibition using the PhenoScanner version 2 database.

701 Table S3. Associations of the variants employed as instruments for SLC13A5 inhibition in the  
702 PhenoScanner version 2 database below the recommended threshold of  $P < 5 \times 10^{-5}$ , which accounts  
703 for multiple testing of the 1490 included genome-wide association studies.

704 Table S4. Inverse-variance weighted Mendelian randomization sensitivity analyses using a pruning  
705 correlation threshold of  $r^2 < 0.01$  for variants employed as instruments. The exposure is genetically  
706 proxied SLC13A5 inhibition, as in the main analysis. This sensitivity analysis is performed for the  
707 primary outcomes, related to kidney traits.

708 Table S5. Results of the genetic colocalisation analysis. H0 signifies the probability that there is no  
709 genetic association in the SLC13A5 gene region with either plasma citrate or the considered  
710 outcome. H1 signifies the probability that there is only an association with plasma citrate. H2  
711 signifies the probability that there is only an association with the outcome. H3 signifies the  
712 probability that there is an association with plasma citrate and the outcome that is attributable to  
713 distinct causal variants. H4 signifies the probability that there is an association with plasma citrate  
714 and the outcome that is attributable to a shared causal variant.

715 Table S6. Metabolome-wide Mendelian randomization analysis investigating the associations of  
716 genetically proxied SLC13A5 inhibition with plasma metabolites. CI: confidence interval.

717 Table S7. Metabolome-wide Mendelian randomization analysis investigating the associations of  
718 genetically proxied SLC13A5 inhibition with urine metabolites. CI: confidence interval.

719 Table S8. Proteome-wide Mendelian randomization analysis investigating the associations of  
720 genetically proxied SLC13A5 inhibition with plasma protein-binding aptamers.

721 Table S9. Phenome-wide association study investigating the associations of a standardised genetic  
722 risk score for SLC13A5 inhibition with clinical outcomes across the phenome.

723 Table S10. Single-nucleotide polymorphisms used as instruments for plasma citrate levels, selected  
724 from throughout the genome. SNP: single-nucleotide polymorphism.

725 Table S11. Metabolome-wide Mendelian randomization analysis investigating the associations of  
726 genetically predicted plasma citrate levels with plasma metabolites. CI: confidence interval.

727 Table S12. Metabolome-wide Mendelian randomization analysis investigating the associations of  
728 genetically predicted plasma citrate levels with urine metabolites. CI: confidence interval.

729 Table S13. Proteome-wide Mendelian randomization analysis investigating the associations of  
730 genetically predicted plasma citrate levels with plasma protein-binding aptamers.

731 Table S14. Phenome-wide association study investigating the associations of a standardised genetic  
732 risk score for plasma citrate with clinical outcomes across the phenome.

733 Table S15. Mendelian randomization statistical sensitivity analyses for biomarkers of renal function,  
734 glucose and lipid metabolism, and inflammation.

735

736 Additional file 3. Figures S1-S6.

737 Figure S1. A scatter plot of genetic association estimates for the SLC13A5 inhibition instrument  
738 variants with plasma citrate (x-axis) and blood urea nitrogen (BUN, y-axis).

739 Figure S2. A scatter plot of genetic association estimates for the SLC13A5 inhibition instrument  
740 variants with plasma citrate (x-axis) and chronic kidney disease (CKD) risk (y-axis).

741 Figure S3. A scatter plot of genetic association estimates for the SLC13A5 inhibition instrument  
742 variants with plasma citrate (x-axis) and creatine-based estimated glomerular filtrate rate (eGFR, y-  
743 axis).

744 Figure S4. A scatter plot of genetic association estimates for the SLC13A5 inhibition instrument  
745 variants with plasma citrate (x-axis) and cystatin C-based estimated glomerular filtrate rate (eGFR, y-  
746 axis).

747 Figure S5. A scatter plot of genetic association estimates for the SLC13A5 inhibition instrument  
748 variants with plasma citrate (x-axis) and microalbuminuria risk (y-axis).

749 Figure S6. A scatter plot of genetic association estimates for the SLC13A5 inhibition instrument  
750 variants with plasma citrate (x-axis) and urine albumin-creatinine ratio (UACR, y-axis).